

Applying principles of robotics to understand the biomechanics, neuromuscular control and clinical rehabilitation of human digits

Francisco J. Valero-Cuevas
Neuromuscular Biomechanics Laboratory
Sibley School of Mechanical and Aerospace Engineering
Cornell University
Ithaca, NY, 14853-7501

Abstract

Given the biomechanical complexity of the human hand, it is not surprising that the grasping ability of individuals after treatment for severe paralysis or injury can seldom be restored to the level of the "normal" hand. Improving clinical outcomes will require i) developing experimental paradigms to evaluate hand function objectively, ii) understanding how the nervous system controls the redundant musculature of the digits, and iii) increasing the clinical impact of computer biomechanical models by validating their anatomical assumptions. Recognizing that the human hand is also a mechanical system, the principles of robotics developed for the analysis of manipulators can be applied to each of these three clinical challenges. This paper is an overview of experimental and theoretical work aimed at understanding individual human digits as serial manipulators.

1.0 Introduction

When restoring biomechanical function to the human digits, as when analyzing or designing electromechanical manipulators, it is useful to define a conceptual paradigm to outline the interactions among components. Figure 1 shows two such paradigms. For an electromechanical manipulator, the mechanical nature of the plant specifies the nature and limits of its grasping capabilities. That is, the laws of mechanics define what grasping function a given manipulator (i.e., plant) can accomplish. Whether and how this function is realized depends on the ability of the controller to interpret the available information (i.e., specifications of the task and feedback signals), implement the appropriate control law, and transmit the command signals to the actuators of the plant. For a biomechanical system such as a human hand, the anatomical structures (articulations, bones, sensory organs and muscles), central nervous system and pinch function are analogous to the plant, controller and grasp function, respectively. One important grasp modality is the two-digit pinch—where the tips of the forefinger and thumb produce the necessary opposing forces to grasp an object.

Two-digit pinch is clinically important because of its usefulness to wheelchair bound individuals such as those with spinal cord injury or stroke [1-5]. Clinicians recognize that wheelchair bound individuals can perform the majority of their activities of daily living with two-digit pinch. Furthermore, the small number of working hand muscles following spinal cord injury (often five or fewer [2, 3, 5]) often precludes the restoration of independent control to more than two digits. By

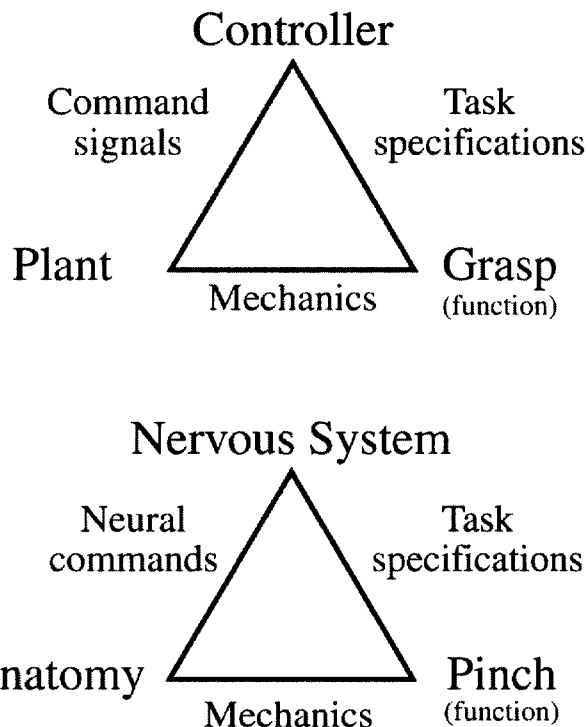


Figure 1. Interactions among components of a generic electromechanical manipulator system (above), and the analog for a biological hand (below).

comparison, the forefinger and thumb have seven and eight muscles each, respectively. In fact, restoring two-digit pinch is often too ambitious for many patients [1]. My research—done in collaboration with hand surgeons, neuroscientists, engineers and physical therapists—is directed towards improving grasping outcomes. As a first step towards this goal, we seek to understand the biomechanics, neuromuscular control and clinical rehabilitation of fingertip force production by human digits—a conceptual and surgical prerequisite to improving the restoration of grasp in general.

2.0 Applications of robotic principles to three challenges in our understanding of fingertip force production

2.1 First obstacle: Mechanical versatility of the human digits

The numerous kinematic degrees-of-freedom (DOF) of the digits and their compliant, high-friction finger pads often allow us to grasp an object using different digit postures (i.e., joint angles) and directing fingertip force differently

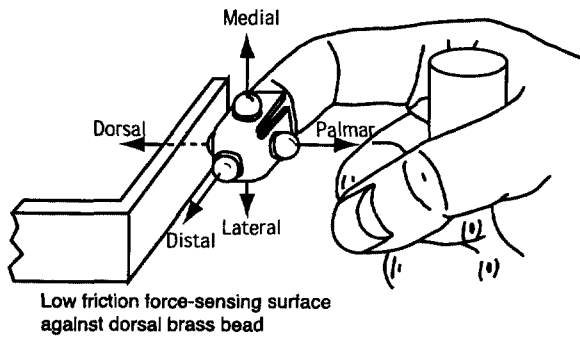


Figure 2. Custom-molded thimble.

(i.e., anywhere within a large friction cone). Ironically, this very versatility can become an important obstacle when designing experimental paradigms to study fingertip force production. Often, the goal of an experiment is to study the choice of muscle coordination strategies when producing fingertip force (see section 2.1 below). However, imprecise force measurement techniques may confound the interpretation of the recorded muscle activity.

We have used robotics principles to design experimental paradigms that clearly define the mechanical task of producing fingertip force with the forefinger for all subjects [6, 7]. Firstly, the posture of the digit during fingertip force production have been standardized as posture specifies the Jacobian matrix—which defines the net joint torques necessary to produce fingertip force in a specific direction. Secondly, the compliant and high-friction interface between the finger pad and dynamometer was eliminated by wearing a thimble—molded to the contour of the distal phalanx—with 5 mm brass beads embedded in locations corresponding to each force direction (Figure 2). Because the forefinger has three flexion DOFs—at the metacarpo-phalangeal (MCP), proximal inter-phalangeal (PIP) and distal inter-phalangeal (DIP) joints—the distal phalanx can impart a torque in the sagittal plane to an object in contact with it (i.e., distal phalanx torque) independently of the fingertip force it can transmit. The low-friction point contact defined by each bead against the force sensing surface required subjects to refrain from producing a distal phalanx torque (otherwise the thimble would rotate about the point of contact). Thirdly, the point contact also required subjects to direct forces within 16° of the surface normal (otherwise the thimble would slip). And lastly, subjects were asked to produce maximal voluntary fingertip force in each direction because parameter optimization theory predicts that a unique coordination pattern is capable of producing maximal force (i.e., the redundancy disappears at the limits of performance, see 2.2). In this way, the nervous systems of all subjects were presented with the same mechanical problem. To shorten the experimental sessions, a programmable robotic arm (Stäubli-Unimate Puma 260, not shown) accurately and quickly positioned the force sensing plate in contact with each brass bead.

2.2 Second obstacle: Muscle redundancy

Human digits are redundant systems to control because they have sufficiently more muscles than kinematic DOFs (i.e., axes of rotation at the articulations). In theory, infinitely many control strategies (implemented as different combinations of muscle forces or coordination patterns) can be used to produce sub-maximal fingertip force in a particular direction [7, 8]. Knowing the extent to which control strategy(ies) of the nervous system are governed by neural synergies (i.e., fixed co-activation of muscles) or mechanical principles will help design effective surgical and rehabilitation procedures.

Unfortunately, we cannot measure directly the control

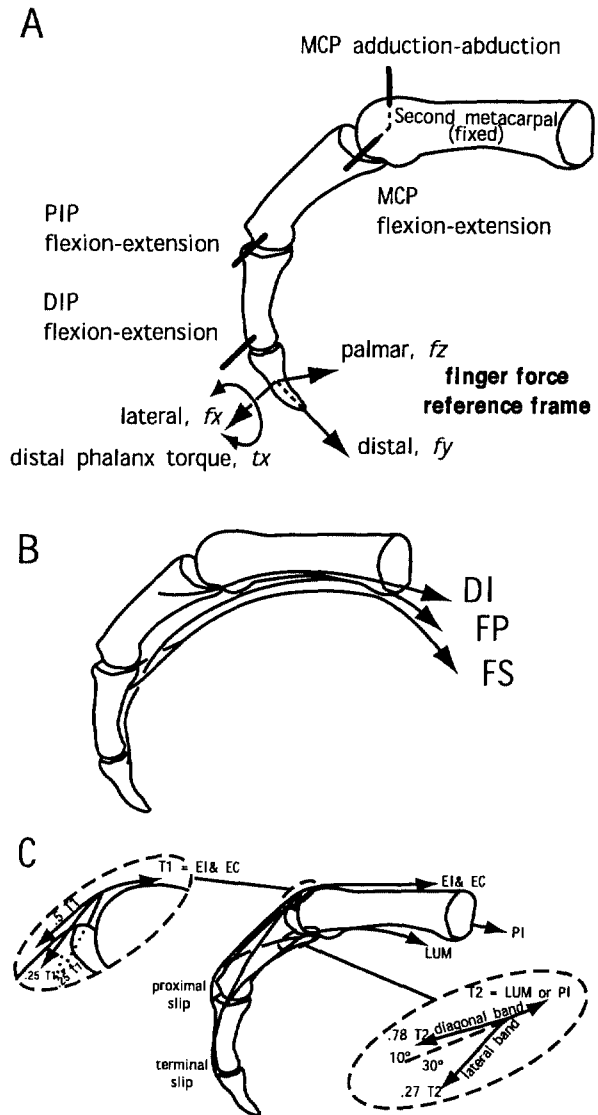


Figure 3. A: Kinematic model of the forefinger. B: Tendon lines of actions of flexor (FP and FS) and dorsal interosseus (DI) muscles. C: Tendon lines of actions of extensor (EI and EC), lumbrical (LUM) and palmar interosseus (PI) muscles. The bifurcation and interconnection of these muscles is called the extensor mechanism of the forefinger.

laws or the command signals the nervous system uses to produce static fingertip force. Imaging of the brain can only infer regions of neural activity [9, 10]. Electrophysiological recordings from neurons, nerves and muscles can only approximate the force command sent to each muscle [11-16]. Importantly, the indirect experimental description of command signals in the nervous system is not sufficient to infer the control strategies in a redundant system. An analytical framework within which to interpret the experimental command signals is desirable.

We used computer biomechanical models based on robotics principles to test the hypothesis that static fingertip forces are produced by mechanically governed control strategies [6, 7]. We tested this hypothesis by comparing coordination patterns predicted using mechanical principles to experimental descriptions of command signals during the production of analogous fingertip forces. The computer model contains a fixed metacarpal and three phalanges articulated by four DOFs (Figure 3A) and is driven by seven independent muscles (Figures 3B & 3C). The torques each muscle produces at all joints spanned by its tendon (i.e., joint torque vector) were calculated based on moment arms measured from a single fresh cadaver [17] and a longitudinally symmetric extensor mechanism (Figure 3C). Isometric force production by each muscle depends on its size, fiber orientation and length [18], and was modeled by scaling its maximal force f_{0i} by its excitation level e_i ($0 \leq e_i \leq 1$) [6, 7].

The computer model is a matrix equation where the static fingertip force production properties of the finger are contained in a 4×7 matrix \mathbf{M} (EQ 1). \mathbf{M} maps a 7-element input vector \mathbf{e} (i.e., muscle excitation pattern) into a 4-element vector $\mathbf{ft} = \{f_x, f_y, f_z, t_x\}^T$ (i.e., their positive directions labeled lateral (f_x), distal (f_y) and palmar (f_z) force, and torque at the distal phalanx (t_x), Figure 3A):

$$\mathbf{ft} = \mathbf{M} \mathbf{e} \quad (1)$$

$$\mathbf{M} = \mathbf{J}^{-T} \mathbf{R} \mathbf{F}_0 \quad (2)$$

\mathbf{M} (EQ 2) is the concatenation of three matrices: the 7×7 \mathbf{F}_0 diagonal matrix of nominal f_{0i} values (scales the excitation level of each muscle into muscle force); the 4×7 \mathbf{R} moment arm and extensor mechanism interaction matrix (superimposes the joint torque vector produced by each muscle force to obtain the net joint torque vector); and the 4×4 \mathbf{J}^{-T} inverse transpose Jacobian matrix of the three-phalanx/four-DOF finger (calculates the \mathbf{ft} produced by the net joint torque vector). The 35 anatomical parameters of \mathbf{M} were either obtained from the literature (3 phalanx lengths, 22 moment arm values, and 7 muscle physiological cross sectional areas) or assumed (3 extensor mechanism parameters due to lack of published material). For a given finger posture and no constraints on \mathbf{e} , \mathbf{M} is a constant non-invertible matrix, i.e., several \mathbf{e} can produce a sub-maximal \mathbf{ft} .

With the bounds on e_i and the constraint $t_x=0$, the unique \mathbf{e} producing the maximal biomechanically feasible

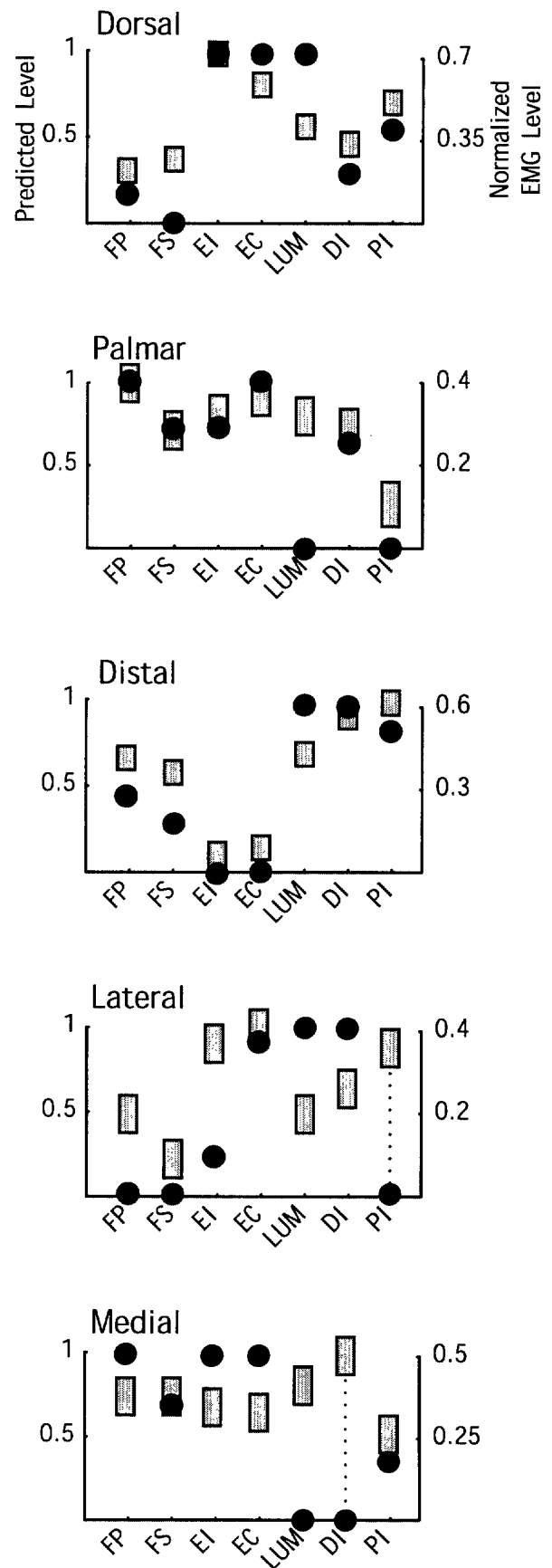


Figure 4. Predicted (circles) and measured (standard error gray bars) coordination patterns for all fingertip force directions.

magnitude of a given \mathbf{ft} was computed geometrically [7, 8]. A muscle excitation pattern \mathbf{e} specifies a point in 7-dimensional “excitation space”(i.e., with as many orthogonal axes as there are muscles, where the excitation of each muscle is a value on the appropriate axis). Because $0 \leq e_i \leq 1$, all achievable \mathbf{e} lie inside a 7-dimensional cube of sides 1 (i.e., unit hypercube). The fourth row of \mathbf{M} specifies how \mathbf{e} is combined to produce distal phalanx torque, t_x . Taking this row as a vector and finding its null-space identifies all excitation patterns that will produce zero distal phalanx torque when mapped through \mathbf{M} , consistent with the experimental task. Using principles of Computational Geometry [19] we calculated the intersection of this null space with the unit hypercube to find the region of excitation space containing all \mathbf{e} that produce \mathbf{ft} with zero distal phalanx torque elements. Finally, mapping the extreme points of this 7-dimensional region through \mathbf{M} produces a convex polyhedron [20] in 3-dimensional output Cartesian “force space” (i.e., $\{f_x, f_y, f_z, 0\}^T$, t_x is zero by construction). The surface of this force polyhedron represents the limits on achievable \mathbf{ft} vectors with zero distal phalanx torque [6, 7, 21, 22]. Thus, a point on the surface of this 3-dimensional polyhedron in force space is produced by a unique excitation pattern, and the distance to the origin specifies the maximal biomechanically achievable magnitude for that static force when $t_x=0$.

This mechanics-based model was successful in reproducing the experimental muscle coordination patterns for palmar, distal and dorsal fingertip forces [6, 7]. That is, the model reproduced the observed use of extensors and absence of PI to produce palmar force (to regulate net joint flexion torques), the absence of extensors for distal force, and the use of LUM, DI and PI (strong MCP flexors) for dorsal force (Figure 4). This agreement for three out of five fingertip force directions suggests the production of large fingertip forces in the plane of finger flexion-extension is governed by mechanical principles. However, the model could not predict the co-activation of DI and PI for lateral and medial fingertip forces (Figure 4). This discrepancy between predicted and measured DI and PI activity may be evidence of a mechanically unnecessary, yet physiologically desirable, strategy to protect the ligaments and capsule of the MCP joint (Long, 1970) from the torsion induced by medial-lateral forces. Alternatively, the assumed model of the MCP joint in the model may be incorrect (See 2.3).

2.3 Third obstacle: Evaluation of assumptions made in biomechanical models.

As shown in 2.2 above, discrepancies between the predictions of a computer model and experimental data can be interpreted to reflect a control strategy of the nervous system. The validity of these interpretations, however, rests on the validity of the assumptions made during the construction of the model. For example, the use of two perpendicular revolute joints to describe the kinematics of the MCP joint naturally make DI and PI an antagonist ad-abduction pair, whose co-activation can

only reduce net ad-abduction torque and lateral force (Model 1 in Figure 5). Thus, it is not surprising that the model would not predict co-activation of DI and PI when asked to maximize medial and lateral fingertip force. However, the MCP joint does not contain any revolute joints. Rather, it is a complex bone-ligament system that can be idealized as behaving like two perpendicular revolute joints for our analytical convenience. Not surprisingly, there exist alternative descriptions of MCP kinematics (Figure 5).

Anatomically, the MCP is known to allow some supination-pronation (i.e., axial rotation) of the proximal phalanx. Long (1970) proposed that this motion is prevented during force production by co-activation of the interossei [14]. More complex kinematic descriptions of the MCP allow such supination-pronation by either tilting the ad-abduction hinge 20° from the vertical (Model 2) [23], or adding a third supination-pronation hinge (Model 3) [24].

Though alternative models incorporating more complex descriptions of the MCP may predict DI and PI co-activation better, the choice of kinematic model also affects force production capabilities. Therefore, as a first step, we used the robotics concept of manipulating force ellipsoids to quantify the effect of different MCP kinematic descriptions on the production of maximal fingertip forces.

Joint torques, $\boldsymbol{\tau}$, are related to forefinger tip forces/torques, \mathbf{ft} , by the inverse transpose Jacobian, \mathbf{J}^{-T} , which is defined by the kinematics of the finger at each finger posture. In the general case,

$$\mathbf{ft} = \mathbf{J}^{-T}\boldsymbol{\tau} \quad (3)$$

where $\mathbf{ft} = \{f_x, f_y, f_z, t_x, t_y, t_z\}^T$, and

$$\boldsymbol{\tau} = \{\tau_1, \dots, \tau_i\}^T, i = \text{number of revolute joints}$$

Assuming every joint torque vector of unit magnitude can be generated, the singular value decomposition (SVD) of \mathbf{J}^{-T} specifies the size and orientation of the manipulating force/torque ellipsoid [25]. The distance from the origin to any point on the surface of the ellipsoid specifies the ease with which fingertip force can be produced in that direction. Our previous work focused on point forces (see sections 2.1 and 2.2). Therefore, we adjusted the manipulating force ellipsoid by using the subset of joint torque vectors belonging to the null-space of the rows of \mathbf{J}^{-T} associated with output torques (i.e., t_x in the case of Model 1). To do this, each axis of the ellipsoid was scaled by the fraction of its corresponding SVD input vector lying in that null-space. This adjusted ellipsoid reflects the relative magnitude of point-forces that can be produced in every direction. Individual muscle forces and moment arms represented by \mathbf{R} and \mathbf{F}_0 matrices in equation 2, should they be considered, would further scale the ellipsoid axes.

For a finger in neutral ad-abduction, the point-force production capabilities in the plane of finger flexion are equal for all models (Figure 6A, Y-Z plane). In the plane perpendicular to finger flexion, Model 2 had greater, and Model 3 had a lesser, lateral force capability than Model 1 (Figure 6B, X-Z plane). Increasing finger flexion greatly increases the lateral force capability of Model 2. Incorporating individual muscle forces and moment arms produces similar results (not shown). Experimental maximal voluntary lateral forces are shown for reference (Figure 6C [6, 7]).

Each MCP description leads to substantially different lateral force capabilities in postures 2 and 3. In Model 1, lateral force capabilities increase moderately with finger flexion, in agreement with experimental data (Figure 6C). In Model 2, the lateral force capabilities increase greatly with finger flexion because the finger tip becomes sufficiently close to the tilted ad-abduction axis, approaching a kinematic singularity. Adding a supination-pronation hinge in Model 3 compromises lateral force production. In postures 2 and 3, supination-pronation torques must be much greater than ad-abduction torque to produce lateral force. Medial-lateral forces decrease because the full ad-abduction capabilities of the digit cannot be used. When the effect of individual muscle forces and moment arms is included, medial-lateral force capability drops well below experimental values (not shown). These results suggest that it is unlikely that finger supination-pronation is an independent kinematic degree-of-freedom.

Fingertip forces induce shear forces at the joints. Idealized kinematic descriptions of joints assume that these shear forces are adequately resisted and will not disarticulate the joint. In reality, every joint is susceptible to disarticulation. Passive bone and ligament structures, and possibly interossei co-activation prevent MCP disarticulation during production of medial-lateral force.

Model 1 may already have an adequate kinematic description of the MCP. Adding active control of joint integrity to it may reproduce the interossei co-activation seen experimentally. However, Model 2 is not invalidated by the fact that experimental medial-lateral forces were not as high as predicted. Subjects may have simply

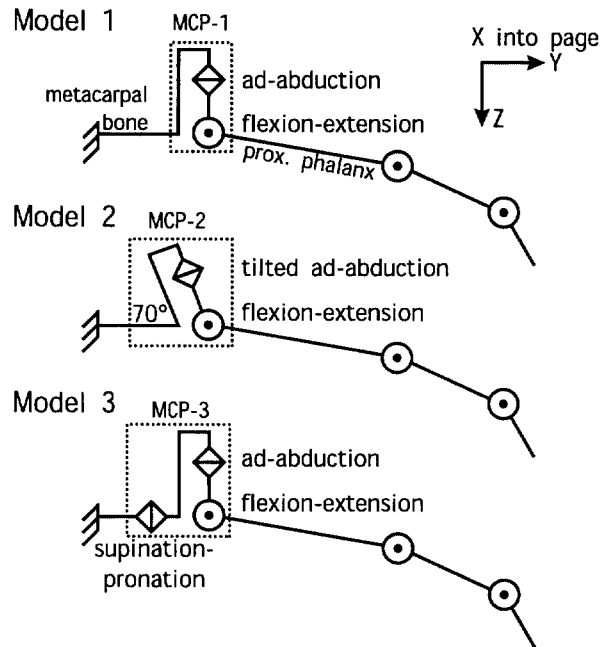


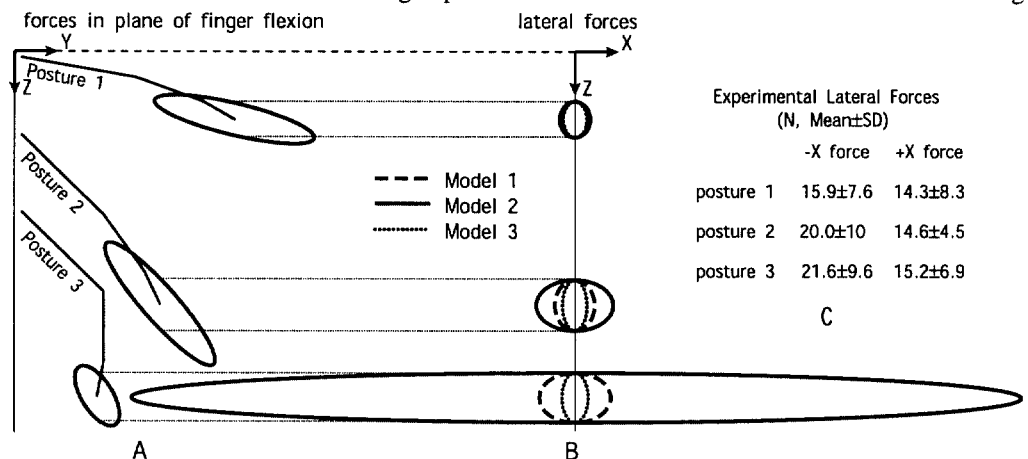
Figure 5. Three alternative descriptions of MCP kinematics in the anatomical literature.

refrained from producing maximal attainable medial-lateral forces to avoid high shear forces at the finger joints, which could lead to injury. More complex finger models that include passive joint structures and monitor MCP integrity may elucidate the role of muscle coordination in enhancing joint stability and preventing injury. However, simpler models may suffice to study forces in the plane of finger flexion-extension (see section 2.2).

3.0 Conclusion

Continuing to design procedures to enhance the manual dexterity of persons with severe neural injuries or orthopedic conditions of the hand will require the collaboration of engineers and clinicians. Fortunately, the conceptual tools roboticists have developed to address the problem of dexterous manipulation have direct application to the problem of functional restoration of grasp in humans. We will continue to work on using

Figure 6. Adjusted manipulating force ellipsoids for the three kinematic models of the MCP joint shown in Figure 5. A: Lateral view. B: Frontal view. C: Experimental values of maximal fingertip forces [6].



these tools to identify anatomical structures critical to grasping function, predict the functional outcome of specific treatments, and develop objective measures of grasping ability to compare pre- and post-treatment function.

References

- [1] V. R. Hentz, J. House, C. McDowell, and E. Moberg, "Rehabilitation and surgical reconstruction of the upper limb in tetraplegia: an update.," *J Hand Surg [Am]*, vol. 17, pp. 964-7, 1992.
- [2] V. R. Hentz, C. Hamlin, and L. A. Keoshian, "Surgical reconstruction in tetraplegia.," *Hand Clin*, vol. 4, pp. 601-7, 1988.
- [3] A. Ejeskar, "Upper limb surgical rehabilitation in high-level tetraplegia," *Hand Clinics*, vol. 4, pp. 585-99, 1988.
- [4] M. W. Keith, P. H. Peckham, G. B. Thrope, K. C. Stroh, B. Smith, J. R. Buckett, K. L. Kilgore, and J. W. Jatich, "Implantable functional neuromuscular stimulation in the tetraplegic hand.," *J Hand Surg [Am]*, vol. 14, pp. 524-30, 1989.
- [5] E. Moberg, "Chapter 116: Surgery for the spastic, stroke and tetraplegic hand.," in *Plastic Surgery*, vol. 8 part 2, J. McCarthy, Ed., First ed. Philadelphia: W.B. Saunders Company, 1990, pp. 4977-4990.
- [6] F. J. Valero-Cuevas, "Muscle coordination of the human index finger," Doctoral Dissertation in the *Mechanical Engineering Department, Biomechanical Engineering Division*. Stanford, CA: Stanford University, 1997.
- [7] F. J. Valero-Cuevas, F. E. Zajac, and C. G. Burgar, "Large index-fingertip forces are produced by subject-independent patterns of muscle excitation.," *Journal of Biomechanics*, vol. 31, pp. 693-703, 1998.
- [8] E. Y. Chao and K. N. An, "Graphical interpretation of the solution to the redundant problem in biomechanics," *Journal of Biomechanical Engineering*, vol. 100, pp. 159-67, 1978.
- [9] Seitz et al. "Somatosensory discrimination of shape: tactile exploration and cerebral activation," *Eur J Neurosci*, vol. 3, pp. 481-492, 1991.
- [10] Kandell and Schwartz, *Principles of neuroscience*, 1991.
- [11] J. V. Basmajian and C. J. De Luca, *Muscles Alive: their functions revealed by electromyography*, 5th ed. Baltimore: Williams & Wilkins, 1985.
- [12] C. G. Burgar, F. J. Valero-Cuevas, and V. R. Hentz, "Fine-wire electromyographic recording during force generation. Application to index finger kinesiologic studies," *Am J Phys Med Rehabil*, vol. 76, pp. 494-501, 1997.
- [13] J. R. Close and C. C. Kidd, "The functions of the muscles of the thumb, the index, and long fingers. Synchronous recording of motions and action potentials of muscles.," *Journal of Bone and Joint Surgery (American)*, vol. 51, pp. 1601-20, 1969.
- [14] C. Long, P. W. Conrad, E. A. Hall, and S. L. Furler, "Intrinsic-extrinsic muscle control of the hand in power grip and precision handling. An electromyographic study.," *J Bone Joint Surg [Am]*, vol. 52, pp. 853-67, 1970.
- [15] M. A. Maier and M. C. Hepp-Reymond, "EMG activation patterns during force production in precision grip. I. Contribution of 15 finger muscles to isometric force.," *Exp Brain Res*, vol. 103, pp. 108-22, 1995.
- [16] M. A. Maier and M. C. Hepp-Reymond, "EMG activation patterns during force production in precision grip. II. Muscular synergies in the spatial and temporal domain.," *Exp Brain Res*, vol. 103, pp. 123-36, 1995.
- [17] K. N. An, Y. Ueba, W. P. Chao, E. Y. Cooney, and R. L. Linscheid, "Tendon excursion and moment arm of index finger muscles," *Journal of Biomechanics*, vol. 16, pp. 419-425, 1983.
- [18] F. E. Zajac, "Muscle and tendon: properties, models, scaling, and application to biomechanics and motor control.," *Crit Rev Biomed Eng*, vol. 17, pp. 359-411, 1989.
- [19] D. Avis and K. Fukuda, "A pivoting algorithm for convex hulls and vertex enumeration of arrangements and polyhedra," *Discrete and Computational Geometry*, pp. 295-313, 1992.
- [20] V. Chvátal, *Linear Programming*. New York: W.H. Freeman and Company, 1983.
- [21] A. D. Kuo and F. E. Zajac, "A biomechanical analysis of muscle strength as a limiting factor in standing posture.," *Journal of Biomechanics*, vol. 26 Suppl 1, pp. 137-50, 1993.
- [22] Y. Kim and S. Desa, "Definition, determination, and characterization of acceleration sets for spatial manipulators.," presented at 21st. Biennial Mechanism Conference, Chicago, Ill., 1990.
- [23] P. Brand and A. Hollister, *Clinical mechanics of the hand*, 2nd ed. St. Louis: Mosby-Year Book, Inc, 1993.
- [24] N. Berme, J. P. Paul, and W. K. Purves, "A biomechanical analysis of the metacarpophalangeal joint.," *Journal of Biomechanics*, vol. 10, pp. 409-412, 1977.
- [25] T. Yoshikawa, *Foundations of robotics: analysis and control*. Cambridge: The MIT Press, 1990.